

2000

A third-order Boussinesq model applied to nonlinear evolution of shallow-water waves

Y. L. Zhang

National University of Singapore

S. P. Zhu

University of Wollongong, spz@uow.edu.au

Publication Details

This article was originally published as Zhang, YL and Zhu, SP, A third-order Boussinesq model applied to nonlinear evolution of shallow-water waves, *Journal of Hydrodynamics*, 12(2), 2000, 107-126. Original article available [here](#).

A third-order Boussinesq model applied to nonlinear evolution of shallow-water waves

Abstract

The conventional Boussinesq model is extended to the third order in dispersion and nonlinearity. The new equations are shown to possess better linear dispersion characteristics. For the evolution of periodic waves over a constant depth, the computed wave envelopes are spatially aperiodic and skew. The model is then applied to the study of wave focusing by a topographical lens and the results are compared with Whalin's (1971) experimental data as well as some previous results from the conventional Boussinesq model. Encouragingly, improved agreement with Whalin's experimental data is found.

Keywords

shallow-water waves, nonlinearity evolution, third-order Boussinesq model

Disciplines

Physical Sciences and Mathematics

Publication Details

This article was originally published as Zhang, YL and Zhu, SP, A third-order Boussinesq model applied to nonlinear evolution of shallow-water waves, *Journal of Hydrodynamics*, 12(2), 2000, 107-126. Original article available [here](#).

A THIRD-ORDER BOUSSINESQ MODEL APPLIED TO NONLINEAR EVOLUTION OF SHALLOW-WATER WAVES

Zhang Ying-long

(CCM-MINDEF, Department of Mech. and Prod. Eng., National University of Singapore, 10 Kent Ridge Crescent, Singapore 119260)

Zhu Song-ping

(Department of Mathematics, the University of Wollongong, Wollongong, NSW 2522, Australia)

ABSTRACT: The conventional Boussinesq model is extended to the third order in dispersion and nonlinearity. The new equations are shown to possess better linear dispersion characteristics. For the evolution of periodic waves over a constant depth, the computed wave envelopes are spatially aperiodic and skew. The model is then applied to the study of wave focusing by a topographical lens and the results are compared with Whalin's (1971) experimental data as well as some previous results from the conventional Boussinesq model. Encouragingly, improved agreement with Whalin's experimental data is found.

KEY WORDS: shallow-water waves, nonlinearity evolution, third-order Boussinesq model

1. INTRODUCTION

In coastal and ocean engineering, the prediction of wave run-up with a desirable accuracy is often of paramount interest. Previously, the second-order Boussinesq model, which assumes that nonlinear and dispersive effects are both weak and of the same order of magnitude, has been extensively used to study the evolution of waves in shallow water (Peregrine, 1967; Mei and Unliata, 1972 etc.). Recently, the conventional Boussinesq model has also been extended to model waves over an intermediate or even large depth, within the scope of a second-order theory (Witting, 1984; Madsen and Sørensen, 1992; Nwogu, 1993; Chen and Liu, 1995; Wei et al., 1995). However, the success of these second-order models is only moderate in some cases; for example, for a topographical lens studied experimentally by Whalin (1971), the results from the aforementioned Boussinesq models are still not very satisfactory even for the least nonlinear case (Liu et al., 1985; Rygg, 1988; Madsen and Sørensen, 1992). We are thus led to believe that higher-order nonlinear and dispersive effects may need to be included in those cases in order to achieve better accuracy.

In this paper, we shall extend the conventional Boussinesq model, which is a second-order model in a perturbation theory (Mei, 1989), to the third order. In particular, we shall derive two equations describing the evolution of a train of weakly nonlinear and dispersive waves over a slowly-varying topography. By taking the higher-order dispersive effects into account, the linear dispersion characteristics of the new equations are shown to be better than those of the conventional Boussinesq equations. To expedite numerical computation, we first derive an approximation for the original elliptic equations using a small-angle parabolic method (Radder, 1979; Liu et al., 1985; Chen and Liu, 1995). We then apply the new model to study the evolution of periodic waves and the generation of higher harmonics over a constant depth. It is found that compared with the results from the conventional Boussinesq model, the results from the new model enhance the spatial aperiodicity and skewness of the envelop, shorten the beat distance (Mei, 1989), and more energy is transferred from lower harmonics to higher harmonics. Then we use the new parabolic equations to study wave focusing by a topographical lens, and compare our results with Whalin's experimental data (1971) and some previous results obtained from the conventional Boussinesq model (Rygg, 1988 etc.). In general, better agreement between the current results and Whalin's data is observed.

2. THE THIRD-ORDER BOUSSINESQ EQUATIONS AND THE PARABOLIC APPROXIMATION

A Cartesian coordinate system $Oxyz$ is adopted with the xOy plane being placed on the undisturbed free surface, the x -axis pointing to the direction of primary wave propagation, and z -axis pointing vertically upwards. Upon choosing a typical time scale ω^{-1} , a typical depth h_0 , and a typical wave amplitude a_0 , the dimensionless variables used to describe the irrotational wave motion of an incompressible inviscid fluid are

$$t' = \omega t, (x', y') = \frac{\omega}{\sqrt{gh_0}}(x, y), z' = \frac{z}{h_0}, h' = \frac{h}{h_0}, \quad (1)$$

where ω is the fundamental angular frequency, $z = \zeta(x, y, t)$ represents the instantaneous position of the free surface, $z = -h(x, y)$ is the stationary bottom profile, (u, v) forms the horizontal velocity vector, g is the gravitational acceleration, and Φ is the velocity

potential. With the primes being dropped from now on for brevity, the dimensionless governing equations and boundary conditions are

$$\Phi_{zz} + \mu^2 \Delta \Phi = 0 \quad (2)$$

$$\Phi_z + \mu^2 \nabla \Phi \cdot \nabla h = 0, \quad z = -h(x, y) \quad (3)$$

$$\left. \begin{aligned} \mu^2(\zeta_t + \varepsilon \nabla \Phi \cdot \nabla \zeta) &= \Phi_z \\ \mu^2(\zeta + \Phi_t) + \frac{\varepsilon}{2}(\Phi_z^2 + \mu^2 |\nabla \Phi|^2) &= 0 \end{aligned} \right\} z = \varepsilon \zeta(x, y, t) \quad (4)$$

where $\mu^2 = \omega^2 h_0 / g$ is a measure of the dispersion effects, $\varepsilon = a_0 / h_0$ is a measure of the nonlinear effects, $\nabla = (\partial / \partial x, \partial / \partial y)$, $\Delta = \nabla \cdot \nabla$ is the two-dimensional Laplacian operator. It is a fundamental assumption in the frame of the Boussinesq theory that $O(\varepsilon) = O(\mu^2) \ll 1$, i.e., the dispersion and nonlinear effects are both weak and of the same order of magnitude. Therefore the Boussinesq theory is only applicable when the ratio of the wavelength and the water depth is sufficiently large (Rygg, 1988; Chen and Liu, 1995).

Following Mei (1989), a perturbation expansion is then carried out to eliminate the z -dependence. Upon keeping terms up to the third order in ε or μ^2 , two coupled equations are obtained. The derivation is standard but very tedious and thus will not be detailed here; the main results are summarized in the Appendix. In particular, upon further assuming that depth variation is small in a typical wavelength, i.e., all derivatives of $h(x, y) \ll O(\mu^2)$ (here and hereafter, we shall use the notation $O(\mu^2)$ etc. as a shorthand of $O(\mu^2, \varepsilon)$ etc., the third-order equations are significantly simplified as (cf. the Appendix)

$$\begin{aligned} \zeta_t + \nabla \cdot (h \nabla \Phi_0) - \mu^2 \left[-\frac{h}{2} \Delta h \zeta_t - h \nabla h \cdot \nabla \zeta_t + \frac{h^2}{2} \Delta (\nabla h \cdot \nabla \Phi_0) + \frac{h^3}{6} \Delta \Delta \Phi_0 \right] \\ + \varepsilon \nabla \cdot (\zeta \nabla \Phi_0) + \frac{\mu^4 h^4}{120} \Delta \Delta \Phi_{0tt} + \frac{\varepsilon \mu^2 h}{2} \nabla \cdot (\zeta \nabla \zeta_t) = O(\mu^6) \end{aligned} \quad (5)$$

$$\begin{aligned} \zeta + \Phi_{0t} - \mu^2 \nabla \cdot \left(\frac{h^2}{2} \nabla \Phi_{0t} \right) + \frac{\varepsilon}{2} |\nabla \Phi_0|^2 + \frac{\mu^4 h^4}{24} \Delta \Delta \Phi_{0t} \\ + \varepsilon \mu^2 (\zeta \zeta_t + \frac{\zeta^2}{2} + \frac{h}{2} \nabla \Phi_0 \cdot \nabla \zeta_t) = O(\mu^6) \end{aligned} \quad (6)$$

where $\Phi_0(x, y, t)$ is the velocity potential evaluated at bottom $z = -h(x, y)$. In this paper, we choose to use Φ_0 and the free-surface elevation ζ , instead of the depth-averaged horizontal velocity vector \vec{u} and ζ as in the conventional Boussinesq equations, as the primary variables.

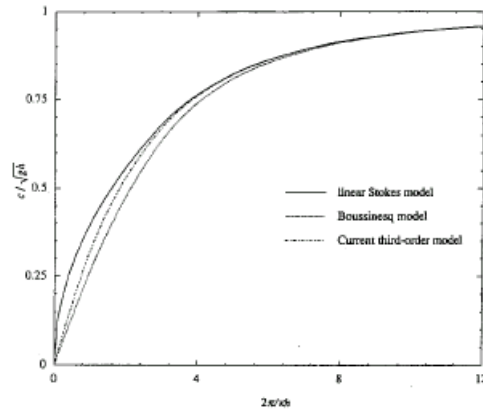


Fig.1 Comparison of linear dispersion relations of the linear Stokes model, $\frac{c^2}{gh} = \frac{\tanh kh}{kh}$, the conventional Boussinesq model, $\frac{c^2}{gh} = (1 + \frac{\kappa^2 h^2}{3})^{-1}$, and the current third-order Boussinesq model, $\frac{c^2}{gh} = (1 + \frac{\kappa^2 h^2}{6})(1 + \frac{\kappa^2 h^2}{2} + \frac{\kappa^4 h^4}{30})^{-1}$

In Fig.1, the linear dispersion relation of the third-order equations is compared with those of the first-order Stokes and the conventional Boussinesq equations. It is

clearly seen that the third-order equations, with the higher-order dispersion having being taken into account, have better linear dispersion characteristics than the conventional Boussinesq equations. According to this figure, it can be applied to a wavelength as short as two times of the typical depth, which is almost as good as the modified Boussinesq equations proposed by Nwogu (1993) and Chen and Liu (1995).

The computational effort required to solve (5) and (6) is still massive, particularly for a large computational domain. Previously, the small-angle parabolic equation method was used by a number of authors (Radder, 1979; Liu et al., 1985; Chen and Liu, 1995) to alleviate the computational effort. Therefore in this paper, we shall adopt the parabolic equation method as well to solve (5) and (6).

Utilizing the following relations:

$$\zeta = -\Phi_{0t} + \frac{\mu^2 h}{2} \Phi_{03t} - \frac{\varepsilon}{2} |\nabla \Phi_0|^2 + O(\mu^4) \quad (7)$$

$$\Delta \Phi_0 = \frac{\Phi_{0tt}}{h} + O(\mu^2) \quad (8)$$

we first combine (5) and (6) into one equation in terms of Φ_0 as

$$\begin{aligned} & \Phi_{0tt} - \nabla \cdot (h \nabla \Phi_0) + \mu^2 \left[-\frac{h^2}{2} \Delta \Phi_{0tt} + \frac{h}{2} \Delta h \Phi_{0tt} + \frac{h^2}{2} \Delta (\nabla h \cdot \nabla \Phi_0) + \frac{h^3}{6} \Delta \Delta \Phi_0 \right] \\ & + \varepsilon [\nabla \Phi_{0t} \cdot \nabla \Phi_0 + \nabla \cdot (\Phi_{0t} \nabla \Phi_0)] + \frac{\mu^4 h^2}{30} \Phi_{06t} + \varepsilon \mu^2 [\Phi_{0t} \Phi_{04t} + 2\Phi_{0t} \Phi_{03t}] \quad (9) \\ & \Phi_{0tt} - \nabla \cdot (h \nabla \Phi_0) + \mu^2 \left[-\frac{h^2}{2} \Delta \Phi_{0tt} + \frac{h}{2} \Delta h \Phi_{0tt} + \frac{h^2}{2} \Delta (\nabla h \cdot \nabla \Phi_0) + \frac{h^3}{6} \Delta \Delta \Phi_0 \right] \\ & + \varepsilon [\nabla \Phi_{0t} \cdot \nabla \Phi_0 + \nabla \cdot (\Phi_{0t} \nabla \Phi_0)] + \frac{\mu^4 h^2}{30} \Phi_{06t} + \varepsilon \mu^2 [\Phi_{0t} \Phi_{04t} + 2\Phi_{0t} \Phi_{03t}] \end{aligned}$$

where Φ_{06t} etc. is a shorthand notation for $\Phi_{0tttttt}$ etc. From Eq. (9), we have

$$\begin{aligned} \Delta \Phi_0 &= \frac{\Phi_{0tt}}{h} - \frac{1}{h} \nabla h \cdot \nabla \Phi_0 - \frac{\mu^2}{3} \Phi_{04t} \\ &+ \frac{\varepsilon}{h} (2 \nabla \Phi_0 \cdot \nabla \Phi_{0t} + \frac{1}{h} \Phi_{0t} \Phi_{0tt}) + O(\mu^4) \quad (10) \end{aligned}$$

$$\begin{aligned} \Delta \Delta \Phi_0 &= \frac{1}{h^2} \Phi_{04t} - \frac{3}{h^2} \nabla h \cdot \nabla \Phi_{0tt} + \Phi_{0tt} \Delta \frac{1}{h} - \frac{2\mu^2}{3h} \Phi_{06t} \\ &- \frac{1}{h} \Delta (\nabla h \cdot \nabla \Phi_0) + \frac{\varepsilon}{h^2} [2(\nabla \Phi_0 \cdot \nabla \Phi_{0t})_{tt} + 2h \Delta (\nabla \Phi_0 \cdot \nabla \Phi_{0t})] \\ &+ \frac{1}{h} (\Phi_{0t} \Phi_{0tt})_{tt} + \Delta (\Phi_{0t} \Phi_{0tt}) + O(\mu^4) \quad (11) \end{aligned}$$

which are substituted into (9) to give

$$\begin{aligned} & \Phi_{0tt} - \nabla \cdot (h \nabla \Phi_0) - \frac{1}{3} \mu^2 h \Phi_{04t} + \varepsilon (2 \nabla \Phi_{0t} \cdot \nabla \Phi_0 + \frac{1}{h} \Phi_{0t} \Phi_{0tt}) \\ & + \mu^2 \left[\frac{h}{2} \Delta h \Phi_{0tt} + \frac{h^2}{3} \Delta (\nabla h \cdot \nabla \Phi_0) + \frac{h^3}{6} \Phi_{0tt} \Delta \frac{1}{h} \right] - \frac{\varepsilon}{h} \Phi_{0t} \nabla h \cdot \nabla \Phi_0 \\ & + \frac{4}{45} \mu^4 h^2 \Phi_{06t} + \varepsilon \mu^2 \left[-3h \nabla \Phi_{0t} \cdot \nabla \Phi_{0tt} - \frac{5}{3} h \nabla \Phi_0 \cdot \nabla \Phi_{03t} \right. \\ & \left. + \frac{h^2}{3} \Delta (\nabla \Phi_0 \cdot \nabla \Phi_{0t}) + \frac{h}{6} \Delta (\Phi_{0t} \Phi_{0tt}) - \frac{1}{6} \Phi_{0t} \Phi_{04t} + \frac{1}{2} \Phi_{0t} \Phi_{03t} \right] \\ & + \varepsilon^2 \left[\frac{1}{2} \nabla \cdot (\nabla \Phi_0 \cdot \nabla \Phi_0) + \frac{2}{h} \Phi_{0t} \nabla \Phi_0 \cdot \nabla \Phi_{0t} + \frac{1}{h^2} \Phi_{0t}^2 \Phi_{0tt} \right] = O(\mu^6) \quad (13) \end{aligned}$$

Since we are seeking for a quasi-steady solution, we decompose Φ_0 and ζ into various modes in terms of the fundamental frequency ω as

$$\zeta = \sum_{n=-\infty}^{\infty} \zeta_n e^{-int} \quad (14)$$

$$\Phi_0 = \sum_{n=-\infty}^{\infty} \varphi_n e^{-int} \quad (15)$$

with the understanding that $(\xi_{-n}, \varphi_{-n}) = (\bar{\xi}_n, \bar{\varphi}_n)$ where the overbars stand for complex conjugate. The amplitudes for the n th harmonic is then $2|\xi_n|$. Note that unlike the case of Stokes waves, the first several higher harmonics may be as large as the first harmonic due to the small phase mismatch (weak dispersion) and resonant interaction between harmonics (Mei, 1989). Therefore we treat all the harmonics as of the same order of magnitude, although harmonics higher than certain order are indeed very small compared to the first harmonic and thus we can truncate the Fourier expansions at a finite n to only include a finite number of harmonics. With the modal decomposition, a system of infinitely many partial differential equations is obtained:

$$\begin{aligned} & -n^2 \varphi_n - \nabla \cdot (h \nabla \varphi_n) - \frac{1}{3} \mu^2 n^4 h \varphi_n + \epsilon \sum_{l=-\infty}^{\infty} \left[-2il \nabla \varphi_l \cdot \nabla \varphi_{n-l} + \frac{il^2(n-l)}{h} \varphi_l \varphi_{n-l} \right] \\ & + \mu^2 \left[-\frac{n^2 h}{2} \Delta h \varphi_n + \frac{h^2}{3} \Delta (\nabla h \cdot \nabla \varphi_n) - \frac{n^2 h^3}{6} \varphi_n \Delta \frac{1}{h} \right] + \frac{i\epsilon}{h} \nabla h \cdot \sum_{l=-\infty}^{\infty} l \varphi_l \nabla \varphi_{n-l} \\ & - \frac{4}{45} \mu^4 n^6 h^2 \varphi_n + \epsilon \mu^2 \left[-3ih \sum_{l=-\infty}^{\infty} l^2 (n-l) \nabla \varphi_l \cdot \nabla \varphi_{n-l} - \frac{5}{3} ih \sum_{l=-\infty}^{\infty} l^3 \nabla \varphi_l \cdot \nabla \varphi_{n-l} \right. \\ & \left. - \frac{ih^2}{3} \sum_{l=-\infty}^{\infty} l \Delta (\nabla \varphi_l \cdot \nabla \varphi_{n-l}) + \frac{ih}{6} \sum_{l=-\infty}^{\infty} l^2 (n-l) \Delta (\varphi_l \varphi_{n-l}) \right] \\ & + \frac{i}{6} \sum_{l=-\infty}^{\infty} l^4 (n-l) \varphi_l \varphi_{n-l} - \frac{i}{2} \sum_{l=-\infty}^{\infty} l^3 (n-l)^2 \varphi_l \varphi_{n-l} \\ & + \epsilon^2 \sum_{l=-\infty}^{\infty} \sum_{m=-\infty}^{\infty} \left\{ \frac{1}{2} \nabla \cdot [(\nabla \varphi_l \cdot \nabla \varphi_m) \nabla \varphi_{n-l-m}] - \frac{2ml}{h} \varphi_l \nabla \varphi_m \cdot \nabla \varphi_{n-l-m} \right. \\ & \left. + \frac{l^2 m (n-l-m)}{h^2} \varphi_l \varphi_m \varphi_{n-l-m} \right\} = O(\mu^6) \end{aligned} \quad (16)$$

As these equations are coupled, the interaction of harmonics and consequently the transfer of energy among harmonics may occur. We shall discuss the cases $n \neq 0$ and $n=0$ separately.

For $n \neq 0$, we can group the terms representing the propagation of a train of unidirectional waves along the x -axis (i.e., the primary propagation direction in this paper) over a constant depth as:

$$\varphi_{nxx} + \frac{1}{h} (n^2 + \frac{1}{3} \mu^2 n^4 h + \frac{4}{45} \mu^4 n^6 h^2) \varphi_n = -\varphi_{nyy} + \frac{1}{h} R_n + O(\mu^6) \quad (17)$$

where

$$\begin{aligned} R_n = & -\nabla h \cdot \nabla \varphi_n + \epsilon \sum_{l=-\infty}^{\infty} \left[-2il \nabla \varphi_l \cdot \nabla \varphi_{n-l} + \frac{il^2(n-l)}{h} \varphi_l \varphi_{n-l} \right] \\ & + \mu^2 \left[-\frac{n^2 h}{2} \Delta h \varphi_n + \frac{h^2}{3} \Delta (\nabla h \cdot \nabla \varphi_n) - \frac{n^2 h^3}{6} \varphi_n \Delta \frac{1}{h} \right] + \frac{i\epsilon}{h} \nabla h \cdot \sum_{l=-\infty}^{\infty} l \varphi_l \nabla \varphi_{n-l} \\ & + \epsilon \mu^2 \left[-3ih \sum_{l=-\infty}^{\infty} l^2 (n-l) \nabla \varphi_l \cdot \nabla \varphi_{n-l} - \frac{5}{3} ih \sum_{l=-\infty}^{\infty} l^3 \nabla \varphi_l \cdot \nabla \varphi_{n-l} \right. \\ & \left. - \frac{ih^2}{3} \sum_{l=-\infty}^{\infty} l \Delta (\nabla \varphi_l \cdot \nabla \varphi_{n-l}) + \frac{ih}{6} \sum_{l=-\infty}^{\infty} l^2 (n-l) \Delta (\varphi_l \varphi_{n-l}) \right] \\ & + \frac{i}{6} \sum_{l=-\infty}^{\infty} l^4 (n-l) \varphi_l \varphi_{n-l} - \frac{i}{2} \sum_{l=-\infty}^{\infty} l^3 (n-l)^2 \varphi_l \varphi_{n-l} \\ & + \epsilon^2 \sum_{l=-\infty}^{\infty} \sum_{m=-\infty}^{\infty} \left\{ \frac{1}{2} \nabla \cdot [(\nabla \varphi_l \cdot \nabla \varphi_m) \nabla \varphi_{n-l-m}] - \frac{2ml}{h} \varphi_l \nabla \varphi_m \cdot \nabla \varphi_{n-l-m} \right. \\ & \left. + \frac{l^2 m (n-l-m)}{h^2} \varphi_l \varphi_m \varphi_{n-l-m} \right\} = O(\mu^2) \end{aligned} \quad (18)$$

From (16) we can see that

$$\Delta\varphi_n = -\frac{n^2}{h}\varphi_n + O(\mu^2) \quad (19)$$

We further assume that the variation along the transverse direction is small, i.e., $\frac{\partial^p \varphi_n}{\partial y^p} = O(\varepsilon^{p/2})$, ($p=1, 2, \dots$) (Chen and Liu, 1995). A small-angle parabolic equation is obtained upon splitting the wave field into a forward and a backward field, i.e., $\varphi_n = \varphi_n^+ + \varphi_n^-$, with

$$\varphi_{nx}^+ = i\kappa_n \varphi_n^+ + T_n \quad (20)$$

$$\varphi_{nx}^- = -i\kappa_n \varphi_n^- - T_n \quad (21)$$

where

$$T_n = \frac{i}{2\kappa_n} \varphi_{ny} + \frac{i\kappa_{nx}}{2\kappa_n^2} \varphi_{nx} - \frac{i}{2\kappa_n h} R_n + O(\mu^6) \quad (22)$$

and the wavenumbers

$$\kappa_n = \frac{n}{\sqrt{h}} \sqrt{1 + \frac{1}{3}\mu^2 n^2 h + \frac{4}{45}\mu^4 n^4 h^2} \quad (23)$$

By neglecting the backward field φ_n^- and dropping “+” for brevity, we obtain a system of infinitely many coupled parabolic equations

$$\varphi_{nx} = i\kappa_n \varphi_n + \frac{i}{2\kappa_n} \varphi_{ny} + \frac{i\kappa_{nx}}{2\kappa_n^2} \varphi_{nx} - \frac{i}{2\kappa_n h} R_n + O(\mu^6) \quad (24)$$

From (24), we obtain

$$\varphi_{nx} = i\kappa_n \varphi_n + O(\mu^2) \quad (25)$$

which, together with (19), can be utilized to simplify R_n

$$\begin{aligned} R_n = & -\nabla h \cdot \nabla \varphi_n + \varepsilon \sum_{l=-\infty}^{\infty} \left[-2il \nabla \varphi_l \cdot \nabla \varphi_{n-l} - \frac{il^2(n-l)}{h} \varphi_l \varphi_{n-l} \right] \\ & + \mu^2 (\alpha_n \varphi_n + \beta_n \varphi_{ny}) + \frac{i\varepsilon}{h} \sum_{l=-\infty}^{\infty} l \varphi_l [ih_x \kappa_{n-l} \varphi_{n-l} + h_y (\varphi_{n-l})_y] \\ & + \varepsilon \mu^2 \sum_{l=-\infty}^{\infty} \gamma_{n,l} \varphi_l \varphi_{n-l} + \varepsilon^2 \sum_{l=-\infty}^{\infty} \sum_{m=-\infty}^{\infty} \delta_{n,l,m} \varphi_l \varphi_m \varphi_{n-l-m} \end{aligned} \quad (26)$$

where

$$\begin{aligned} \alpha_n = & -\frac{n^2 h}{2} \Delta h - \frac{2}{3} \kappa_n^2 h^2 h_{xx} + \frac{i}{3} \kappa_n h^2 (\Delta h_x - n^2 \frac{h_x}{h}) \\ & - \frac{n^2 h^3}{6} \Delta \frac{1}{h} = O(\mu^2) \end{aligned} \quad (27)$$

$$\beta_n = \Delta h_y - n^2 \frac{h_y}{h} + 4i\kappa_n h_{xy} = O(\mu^2) \quad (28)$$

$$\begin{aligned} \gamma_{n,l} = & h\kappa_n \kappa_{n-l} \left[\frac{8}{3} il^2 n - il^3 - \frac{(n-l)^2}{3} - \frac{l^2}{3} - \frac{2}{3} h\kappa_n \kappa_{n-l} \right] \\ & - \frac{i}{6} (n-l)^2 l^2 (n+2l) \end{aligned} \quad (29)$$

$$\begin{aligned} \delta_{n,l,m} = & \frac{\kappa_l \kappa_m}{2} \left[\kappa_l \kappa_{n-l-m} + \kappa_m \kappa_{n-l-m} + \frac{(n-l-m)^2}{h} \right] \\ & + \frac{2lm}{h} \kappa_m \kappa_{n-l-m} + \frac{l^2 m (n-l-m)}{h^2} \end{aligned} \quad (30)$$

By collecting x and y derivatives in (24), we finally have

$$\varphi_{nx} = \frac{i\kappa_n}{G_n}\varphi_n + \frac{i}{2\kappa_n G_n}\varphi_{nxy} - \frac{i}{2\kappa_n G_n h}W_n + O(\mu^6) \quad (31)$$

where

$$G_n = 1 - \frac{i\kappa_{xy}}{2\kappa_n^2} - \frac{ih_x}{2\kappa_n h} \quad (32)$$

$$\begin{aligned} W_n &= (\mu^2\beta_n - h_y)\varphi_{ny} + \mu^2\alpha_n\varphi_n + \epsilon \sum_{l=-\infty}^{\infty} [-2il\nabla\varphi_l \cdot \nabla\varphi_{n-l} + \frac{il^2(n-l)}{h}\varphi_l\varphi_{n-l}] \\ &+ \frac{i\epsilon}{h} \sum_{l=-\infty}^{\infty} l\varphi_l [ih_x\kappa_{n-l}\varphi_{n-l} + h_y(\varphi_{n-l})_y] \\ &+ \epsilon\mu^2 \sum_{l=-\infty}^{\infty} \gamma_{n,l}\varphi_l\varphi_{n-l} + \epsilon^2 \sum_{l=-\infty}^{\infty} \sum_{m=-\infty}^{\infty} \delta_{n,l,m}\varphi_l\varphi_m\varphi_{n-l-m} \end{aligned} \quad (33)$$

For $n=0$, since in this paper we are only concerned with linear incident waves containing only the first harmonic, φ_0 and ξ_0 are second-order quantities which represent the mean “set-down”. The corresponding parabolic equation can be derived directly from (5) and (6) by keeping terms up to the order μ^4 as

$$\nabla\varphi_0 = -\frac{i\epsilon}{h} \sum_{l=-\infty}^{\infty} l\varphi_l\nabla\varphi_{-l} + O(\mu^4) \quad (34)$$

Note that since φ_0 does not appear in the zeroth-order terms in (31), only the terms of order higher than μ^4 have to be kept in (34). The x-component of (34)

$$\varphi_{0x} = -\frac{i\epsilon}{h} \sum_{l=-\infty}^{\infty} l\varphi_l(\varphi_{-l})_x + O(\mu^4) \quad (35)$$

supplies the needed parabolic equation for $n=0$. This equation coupled with (31) through the nonlinear terms.

So far we have obtained a system of parabolic equations for all harmonics. For numerical computation, we further factor out the fast-varying component of φ_n as

$$\varphi_n = \psi_n e^{i\hat{\kappa}_n x} \quad (36)$$

where $\hat{\kappa}_n$ is a series of reference wavenumbers at a reference depth h_1 , i. e., $\hat{\kappa}_n = \frac{n}{\sqrt{h_1}}$
 $\sqrt{1 + \frac{1}{3}\mu^2 n^2 h_1 + \frac{4}{45}\mu^4 n^4 h_1^2}$. The equations for ψ_n are

• for $n=0$,

$$\psi_{0x} = -\frac{i\epsilon}{h} \sum_{l=-\infty}^{\infty} l\psi_l [(\psi_{-l})_x + i\hat{\kappa}_{-l}\psi_{-l}] + O(\mu^4) \quad (37)$$

• for $n \neq 0$,

$$\psi_{nx} = i\left(\frac{\kappa_n}{G_n} - \hat{\kappa}_n\right)\psi_n + \frac{i}{2\kappa_n G_n}\psi_{nxy} - \frac{i}{2\kappa_n G_n h}W'_n + O(\mu^6) \quad (38)$$

where

$$\begin{aligned}
W'_n &= (\mu^2 \beta_n - h_y) \psi_{ny} + \mu^2 \alpha_n \psi_n + \varepsilon \sum_{l=-\infty}^{\infty} e^{i(\hat{\kappa}_l + \hat{\kappa}_{n-1} - \hat{\kappa}_n)x} \\
&\times \{-2il[(\psi_l)_x (\psi_{n-l})_x + (\psi_l)_y (\psi_{n-l})_y + i\hat{\kappa}_{n-1}(\psi_l)_x \psi_{n-l} + i\hat{\kappa}_l \psi_l (\psi_{n-l})_x]\} \\
&+ \left[2i\hat{\kappa}_n \hat{\kappa}_{n-l} + \frac{i\hat{\kappa}_n^2(n-l)}{h}\right] \psi_l \psi_{n-l} + \frac{i\varepsilon}{h} \sum_{l=-\infty}^{\infty} l \psi_l e^{i(\hat{\kappa}_l + \hat{\kappa}_{n-1} - \hat{\kappa}_n)x} \\
&\times [ih_x \hat{\kappa}_{n-l} \psi_{n-l} + h_y (\psi_{n-l})_y] + \varepsilon \mu^2 \sum_{l=-\infty}^{\infty} \gamma_{n,l} \psi_l \psi_{n-l} e^{i(\hat{\kappa}_l + \hat{\kappa}_{n-1} - \hat{\kappa}_n)x} \\
&+ \varepsilon^2 \sum_{l=-\infty}^{\infty} \sum_{m=-\infty}^{\infty} \delta_{n-l,m} \psi_l \psi_m \psi_{n-l-m} e^{i(\hat{\kappa}_l + \hat{\kappa}_m + \hat{\kappa}_{n-1-m} - \hat{\kappa}_n)x}
\end{aligned} \tag{39}$$

The range of applicability of the parabolic method can be estimated by comparing the linear dispersion characteristics of the original equations and the parabolic equations, i. e., upon substituting $\frac{g}{8-115. \text{gr}}$ and $h=\text{const.}$ into the linearized versions of (17) and (24). Interestingly, the resulting equations for κ_x and κ_y

$$\begin{aligned}
\kappa_x^2 + \kappa_y^2 &= \kappa_n^2 \tag{40} \\
\kappa_x &= \kappa_n - \frac{\kappa_n^2}{2\kappa_n} \tag{41}
\end{aligned}$$

are identical with those of Chen and Liu (1995) or for the mid-slope equation; they seem to be inherent from the methodology itself, and give an excellent interpretation for the name “parabolic method”, i. e., using a parabola to approximate an ellipse. Therefore the current parabolic model is applicable if the angle of scattering is no greater than 30° .

The Crank-Nicholson method was adopted to solve (37) and (38) numerically. It employs central difference in both x and y directions. When marching with x, which is a time-like variable, the collocation points were located in the middle of the two levels (Greenspan and Casulli, 1988). The linear version of the Crank-Nicholson method is unconditionally stable. As stated before, the summations were truncated to include only $(2N+1)$ harmonics (Ψ_{-N}, \dots, Ψ_N). A Newton-Raphson method was used to solve the nonlinear complex system and the nonlinear iterations were found to converge very fast (within no more than four iterations for all the problems treated in this paper); on the other hand, the simple iteration scheme proposed by Liu et al. (1985) was found to converge very slowly (up to more than 100 iterations needed). In the numerical computation, we treated Ψ_j and Ψ_{-j} as independent unknowns in order to facilitate the use of the Newton-Raphson method. An IMSL subroutine LSLCG was employed to invert the complex Jacobian. At the starting point of x, an initial condition derived from the linearized version of (5) and (6), with the assumption that only the first harmonic is present there, was imposed for the sake of compatibility.

The number of harmonics included will affect the numerical accuracy unless it is sufficiently large. $N=8$ was found to be sufficient for all the problems dealt with in this paper. An example of the convergence test is shown in Fig.2, in which the most nonlinear case in Whalin's (1971) experiment (see §3.2) is examined. The comparison indicates that including more than 8 harmonics will not significantly affect the first three harmonics which are of primary interest here. On the other hand, the results with $N=6$ were still quite different from those with $N=8$ in the lee region; the results with N being less than 8 may not be reliable in this case.

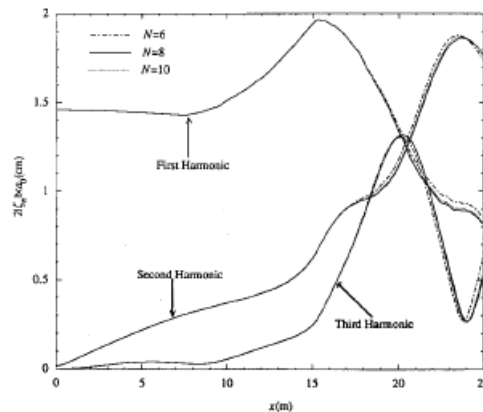


Fig.2 Convergence test for a case in Whalin's experiments with $T=3s$ and $a_0=1.46\text{cm}$

After ψ_n is solved, each harmonic component of the free-surface elevation is calculated from

$$\zeta = \sum_{n=-\infty}^{\infty} \zeta_n e^{i(\hat{\kappa}_n x - n t)} \quad (42)$$

$$\begin{aligned} \zeta_n = & in(1 + \frac{1}{2}\mu^2 n^2 h + \frac{5}{24}\mu^4 n^4 h^2)\psi_n - \frac{i\mu^2 nh}{2}[h_x(\psi_{nx} + i\hat{\kappa}_n \psi_n) + h_y(\psi_n)_y] \\ & - \frac{\epsilon}{2} \sum_l e^{i(\hat{\kappa}_l + \hat{\kappa}_{n-l} - \hat{\kappa}_n)x} [(\psi_l)_x + i\hat{\kappa}_l \psi_l][(\psi_{n-l})_x + i\hat{\kappa}_{n-l} \psi_{n-l}] \\ & + (\psi_l)_y (\psi_{n-l})_y + \epsilon \mu^2 \sum_l [hl(n + l/2)\hat{\kappa}_l \hat{\kappa}_{n-l} \end{aligned} \quad (43)$$

3. NUMERICAL RESULTS AND DISCUSSIONS

3.1 Constant depth

It has long been known that higher harmonics are resonated as a train of initially periodic waves evolves over a constant but shallow water depth due to the nonlinearity and the weak dispersion effects (Mei, 1989). The generation of higher harmonics makes the wave profile significantly different from that of simple harmonic waves; it becomes skew and asymmetric and even aperiodic (Madsen et al., 1970). Secondary crests are generally quite appreciable. Since the current third-order model incorporates higher-order nonlinearity and dispersion, higher harmonics are expected to grow faster than those in the conventional second-order Boussinesq model. Fig.3 shows an example of the evolution of long waves over a constant depth with $\mu^2=0.05$ and $\epsilon=0.02$. One can see clearly from this figure that with the third-order model, there is more energy exchange between harmonics and the second and third harmonics are excited to a slightly higher amplitude. Another conspicuous distinction between the results from the conventional Boussinesq model and the third-order model is that the latter are obviously skew and aperiodic especially for the second and third harmonics. Since some envelopes are spatially aperiodic here, we define the beat distance as the distance between two neighboring minimum amplitudes. It is seen from Fig.3 that the beat distance is also shorter in the new model. It is about 105, which compares well with 100 according to the two-harmonics interaction theory (Mei, 1989). The discrepancy is mainly due to the fact that the formula in Mei (1989, pp.591) is only applicable for a large Ursell number $\mu r = \epsilon \mu^2$.

From this comparison and taking into consideration the fact that the first-order linear model (long-wave equation) predicts no higher harmonics, we deduce that including higher-order nonlinearity and dispersion effects will lead to more energy exchange between harmonics within a shorter distance, and destroy the spatial periodicity.

3.2 Whalin's topographical lens

Whalin (1971) conducted a series of wave focusing experiments in a wave tank of 25.603m long and 6.096m wide. Eleven semi-circular steps were placed along the channel from $x=7.63m$ to $x=15.25m$ (cf. Rygg, 1988). He also gave an equation approximating the topography

$$h(x, y) = \begin{cases} 0.4572, & 0 \leq x \leq 10.67 - G(y) \\ 0.4572 + \frac{1}{25}(10.67 - G - x), & 10.67 - G(y) \leq x \leq 18.29 - G(y) \\ 0.1524, & 18.29 - G(y) \leq x \leq 21.34 \end{cases} \quad (44)$$

where

$$G(y) = \sqrt{y(6.096 - y)} \quad (45)$$

All the length variables in (44) and (45) are measured in meters. For this topography, the variation of the bottom is indeed very small. Several incident waves with different periods $T=1.0, 2.0$ and $3.0s$ and steepness are generated by a wavemaker installed at the deeper portion of the channel with $h=0.4572m$. The estimation of various dimensionless quantities can be found in Liu and Tsay (1984) and Rygg (1988).

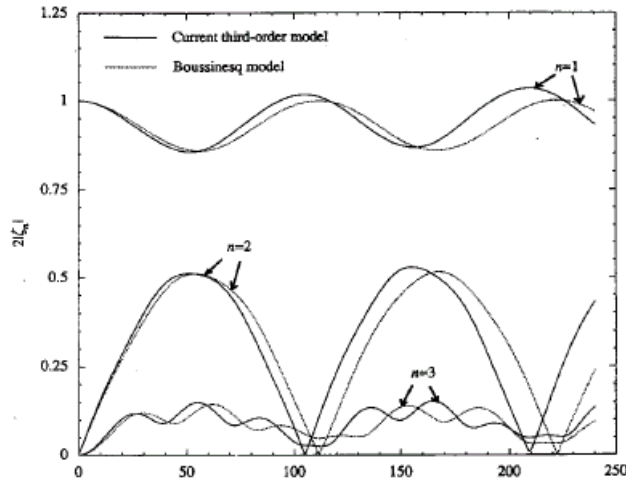
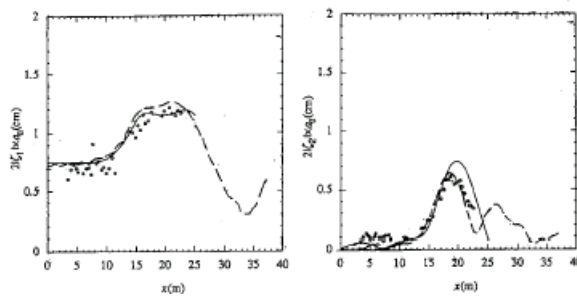


Fig.3 Evolution of long waves over a constant depth, with the grid size $\Delta x=0.4$, and $N=6$

We adopt the same topography in order to test and compare our results with previously obtained ones. In the numerical computation, different grid sizes were tested for the convergence of the numerical scheme and the results presented here were obtained with a grid size $\Delta x=0.125\text{m}$ and $\Delta y=0.1524\text{m}$ in terms of the dimensional variables. The CPU time spent on each x-step was about 36s on a SUN 4/470 Sparc Server when eight harmonics were included.

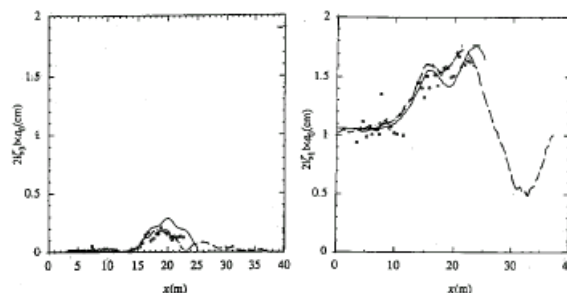
The nonlinear diffraction-refraction of the incident waves over the topographical lens has been studied by a number of authors using second-order (in μ^2 of ϵ) models. Liu and Tsay (1984) produced the results for $T=1$, 2s with a second-order Stokes theory. The results for $T=3\text{s}$ were later obtained by Liu et al. (1985) using the parabolic approximation of the conventional Boussinesq model and the Kadomtsev Petviashvili (KP) equation. Rygg (1988) solved the elliptic Boussinesq equations directly in a time domain and obtained results for $T=2, 3\text{s}$. His results were found to be in close agreement with those of Madsen and Sørensen (1992) and Chen and Liu (1995), who proposed extended (but still second-order) Boussinesq equations with better linear characteristics, and claimed to be able to simulate all cases. However, all these models suffer from a common drawback; the model predictions to Whalin's experiment are still not satisfactory, ever for the least nonlinear cases. In particular, the first harmonics always seem to have been significantly overestimated in the intermediate and long wave cases $T=2, 3\text{s}$.



4(a) First harmonic

4(b) Second harmonic

Fig.4 Comparison of amplitudes of the first three harmonics among the results from the third-order model (solid lines), the conventional Boussinesq model by Rygg (1988) (dash lines), and Whalin's experiments (circles) for $T=2.0\text{s}$ and $a_0=0.75\text{cm}$

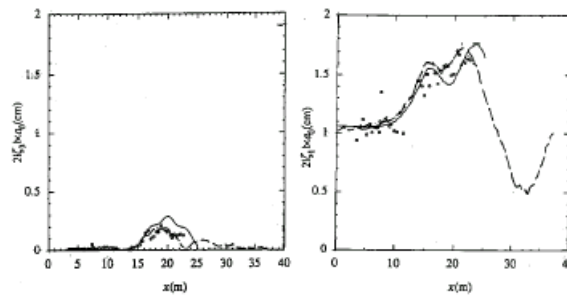


4(c) Third harmonic

5(a) First harmonic

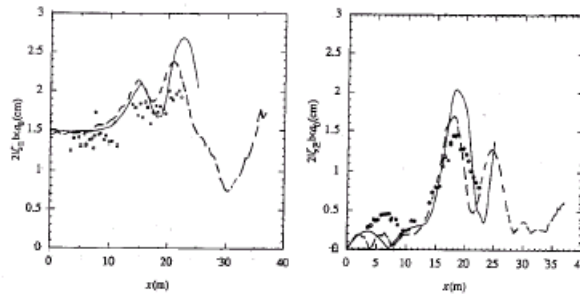
Fig.5 Comparison of amplitudes of the first three harmonics among the results from the

third-order model (solid lines), the conventional Boussinesq model by Rygg (1988) (dash lines), and Whalin' s experiments (circles) for $T=2.0s$ and $a_0=1.06cm$



5(b) Second harmonic

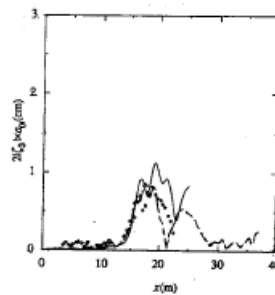
5(c) Third harmonic



6(a) First harmonic

6(b) Second harmonic

Fig.6 Comparison of amplitudes of the first three harmonics among the results from the third-order model (solid lines), the conventional Boussinesq model by Rygg (1988) (dash lines), and Whalin' s experiments (circles) for $T=2.0s$ and $a_0=1.49cm$

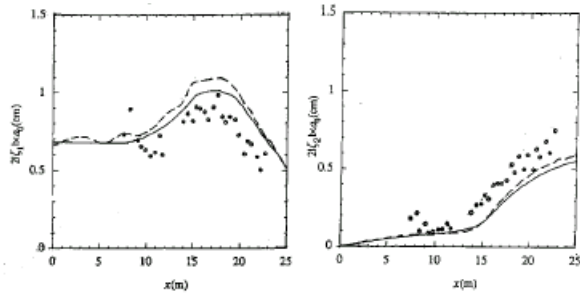


6(c) Third harmonic

The short wave case $T=1s$ was excluded from our study since it has an Ursell number around 0.2 which is too small for the current third-order Boussinesq model. The results for $T=2, 3s$ are shown in Figs. 4-9. Compared to the models of Liu and Tsay (1984) and Liu et al. (1985), Rygg' s model does seem to have made some improvement for the second and third harmonics, particularly with the sharp maximum for the amplitude of the second harmonics for $T=2s$ being reproduced. However, the improvement on the first harmonics does not seem to be so significant. Compared to Rygg' s results from the conventional Boussinesq model, the first harmonics are generally better estimated by the current model for $T=2s$ (Figs. 4a, 5a and 6a), except that for the most nonlinear case $a_0=1.49cm$ (Fig.6a), there is a small portion of the focal zone where the current estimation is worse than that shown in Rygg (1988). The overestimation is believed to be a result of the deficiency of the parabolic approximation. As noted by Rygg (1988), three-dimensional effects can be important in the focusing region; better results would have been obtained if the full elliptic equations had been solved. Nevertheless, the fact that the results from the current third-order have followed the experimental data much more closely and within a much larger range compared to those in Rygg (1988) made us believe that neglecting the frictional dissipation may not be the reason for the conventional Boussinesq model to yield an overestimation for the first harmonic amplitude, as Rygg conjectured. The inclusion of the third-order effects seems to have corrected that overestimation to a large extent.

Similar overestimation in this region is also observed for the second and third harmonics (Figs. 4-6 (b)-(c)), but otherwise our results are generally in good agreement with those of

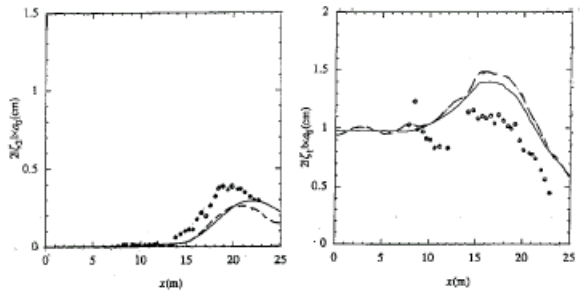
Rygg (1988) and Whalin (1971); the trend of the experimental data is well captured. Comparison of our results and those from the conventional Boussinesq model clearly indicates that more energy transfer between the harmonics occurs when the higher-order dispersion and nonlinear effects are taken into account.



7(a) First harmonic

7(b) Second harmonic

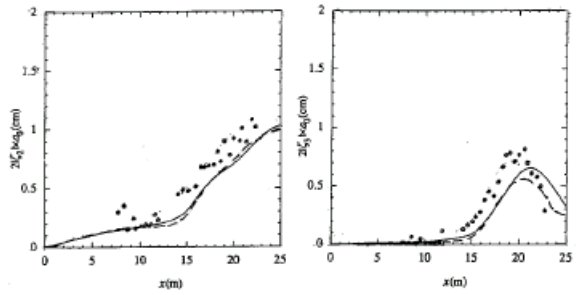
Fig.7 Comparison of amplitudes of the first three harmonics among the results from the third-order model (solid lines), the conventional Boussinesq model by Rygg (1988) (dash lines), and Whalin' s experiments (circles) for T=3.0s and a0=0.68cm



7(c) Third harmonic

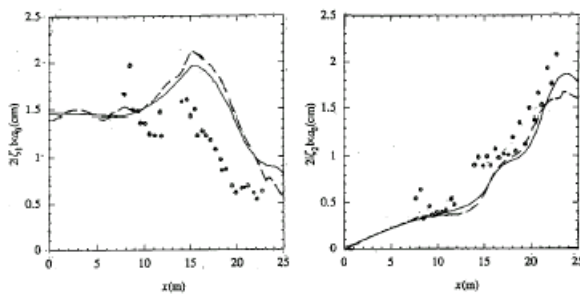
8(a) First harmonic

Fig.8 Comparison of amplitudes of the first three harmonics among the results from the third-order model (solid lines), the conventional Boussinesq model by Rygg (1988) (dash lines), and Whalin' s experiments (circles) for T=3.0s and a0=0.98cm



8(b) Second harmonic

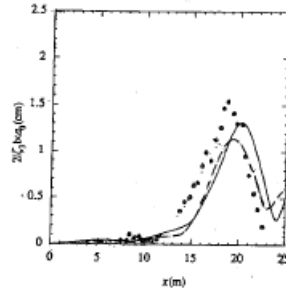
8(c) Third harmonic



9(a) First harmonic

9(b) Second harmonic

Fig.9 Comparison of amplitudes of the first three harmonics among the results from the third-order model (solid lines), the conventional Boussinesq model by Rygg (1988) (dash lines), and Whalin' s experiments (circles) for T=3.0s and a0=1.46cm



9(c) Third harmonic

Similar conclusions can be drawn for the longer incident wave $T=3s$ (Figs. 7-9). In this case, however, the maxima and minima of the second and third harmonics seem to have been better predicted with the current model except in Fig.7b where the amplitude of the second harmonic from the current model is slightly smaller than that from the conventional Boussinesq model in the focusing region. Results from both Rygg' s- model and our model seem to have underestimated the amplitudes of the second and third harmonics. It is interesting for us to notice that there is a clear phase shift in the amplitudes of the second and third harmonics between the results from (the second- or third-order) Boussinesq models and the experimental data; without this phase shift, the agreement would have been dramatically improved. But in general, with our new model improved results are obtained for the first harmonic amplitudes, while the results for the second and third harmonics agree well with Rygg' s results and are in reasonable agreement with the experimental data.

4 CONCLUSIONS

A third-order Boussinesq model is proposed and is shown to possess better linear dispersion characteristics than the conventional Boussinesq model. With the higher-order dispersion and nonlinear effects being incorporated, it is found that more energy is exchanged between harmonics within a shorter distance. For the evolution of long waves over a constant depth, the inclusion of the higher-order dispersion and nonlinear effects seems to induce skewness in the wave envelop, increase the amplitudes for the higher harmonics, and destroy the spatial periodicity. A parabolic equation method is applied to the new third-order equations, resulting in a system of coupled parabolic equations describing the interaction of harmonics. Numerical results are presented for wave focusing over a topographical lens. Compared to previous results from the conventional Boussinesq model, improved agreement with the experimental data, especially for the first harmonics, is observed.

APPENDIX: THIRD-ORDER BOUSSINESQ EQUATIONS

With a Taylor expansion for Φ at $z=-h(x, y)$

$$\Phi = \sum_{n=0}^{\infty} (\varepsilon + h)^n \Phi_n \quad (A1)$$

where Φ_n can be calculated from the bottom boundary condition, and keeping terms up to $O(\mu^6)$, the satisfaction of the two free-surface boundary conditions in (4) leads to the third-order Boussinesq equations

$$\begin{aligned} & \zeta_t + \nabla \cdot (h \nabla \Phi_0) - \mu^2 \left[|\nabla h|^2 \nabla h \cdot \nabla \Phi_0 + h \Gamma_1 \Phi_0 + \frac{h^2}{2} \Gamma_3 \Phi_0 + \frac{h^3}{6} \Delta \Delta \Phi_0 \right] \\ & + \varepsilon \nabla \cdot (\zeta \nabla \Phi_0) + \mu^4 \left[|\nabla h|^4 \nabla h \cdot \nabla \Phi_0 + h \Gamma_2 \Phi_0 + \frac{h^2}{2} \Gamma_4 \Phi_0 + \frac{h^3}{6} \Gamma_5 \Phi_0 \right. \\ & \left. + \frac{h^4}{24} \Gamma_6 \Phi_0 + \frac{h^4}{120} \Delta \Delta \Phi_{0t} \right] - \varepsilon \mu^2 \left[\nabla \zeta \cdot \left(\nabla \nabla \cdot \left(\frac{h^2}{2} \nabla \Phi_0 \right) \right) \right. \\ & \left. + \zeta \Gamma_1 \Phi_0 + h \zeta \Gamma_3 \Phi_0 + \frac{\zeta h^2}{2} \Delta \Delta \Phi_0 \right] O(\mu^6) \end{aligned} \quad (A2)$$

$$\begin{aligned} & \zeta + \Phi_{0t} - \mu^2 \nabla \cdot \left(\frac{h^2}{2} \nabla \Phi_{0t} \right) + \frac{\varepsilon^2}{2} |\nabla \Phi_0|^2 + \mu^4 \left(h |\nabla h|^2 \nabla h \cdot \nabla \Phi_{0t} + \frac{h^2}{2} \Gamma_1 \Phi_{0t} \right. \\ & \left. + \frac{h^3}{6} \Gamma_3 \Phi_{0t} + \frac{h^4}{24} \Delta \Delta \Phi_{0t} \right) + \varepsilon \mu^2 \left[-\zeta \nabla \cdot (h \nabla \Phi_{0t}) + \frac{1}{2} (\nabla \cdot (h \nabla \Phi_0))^2 \right. \\ & \left. - \nabla \Phi_0 \cdot \left(\nabla \nabla \cdot \left(\frac{h^2}{2} \nabla \Phi_0 \right) \right) \right] O(\mu^6) \end{aligned} \quad (A3)$$

where the linear operators $\Gamma_i (i=1, \dots, 6)$ are defined as

$$\Gamma_1 f = (\nabla h \cdot \nabla f) \Delta h + 2 \nabla h \cdot \nabla (\nabla h \cdot \nabla f) + |\nabla h|^2 \Delta f \quad (A4)$$

$$\begin{aligned} \Gamma_2 f = & |\nabla h|^4 \Delta h + 2 |\nabla h|^2 \Delta h (\nabla h \cdot \nabla f) + 2 |\nabla h|^2 \nabla h \cdot \nabla (\nabla h \cdot \nabla f) \\ & + 2 \nabla h \cdot \nabla (|\nabla h|^2 \nabla h \cdot \nabla f) \end{aligned} \quad (A5)$$

$$\Gamma_3 f = \Delta h \Delta f + 2 \nabla h \cdot \nabla \Delta f + \Delta (\nabla h \cdot \nabla f) \quad (A6)$$

$$\begin{aligned} \Gamma_4 f = & (\Delta h)^2 (\nabla h \cdot \nabla f) + 2 \Delta h [\nabla h \cdot \nabla (\nabla h \cdot \nabla f)] + 2 |\nabla h|^2 \Delta h \Delta f \\ & + \Delta (|\nabla h|^2 \nabla h \cdot \nabla f) + 2 \nabla h \cdot \nabla (\Delta h \nabla h \cdot \nabla f) + 4 \nabla h \cdot \nabla [\nabla h \cdot \nabla (\nabla h \cdot \nabla f)] \end{aligned} \quad (A7)$$

$$\begin{aligned} \Gamma_5 f = & (\Delta h)^2 \Delta f + 2 \Delta h \nabla h \cdot \nabla \Delta f + \Delta h \Delta (\nabla h \cdot \nabla f) + 2 \nabla h \cdot \nabla (\Delta h \Delta f) \\ & + 4 \nabla h \cdot \nabla (\nabla h \cdot \nabla \Delta f) + 2 \nabla h \cdot \nabla \Delta (\nabla h \cdot \nabla f) + |\nabla h|^2 \Delta \Delta f \\ & + \Delta (\Delta h \nabla h \cdot \nabla f) + 2 \Delta [\nabla h \cdot \nabla (\nabla h \cdot \nabla f)] + \Delta (|\nabla h|^2 \Delta f) \end{aligned} \quad (A8)$$

$$\begin{aligned} \Gamma_6 f = & \Delta h \Delta \Delta f + 2 \nabla h \cdot \nabla \Delta \Delta f + \Delta (\Delta h \Delta f) + 2 \Delta (\nabla h \cdot \nabla \Delta f) \\ & + \Delta \Delta (\nabla h \cdot \nabla f) \end{aligned} \quad (A9)$$

Eqs. (A2) and (A3) are valid for an arbitrary depth variation $\nabla h = O(1)$. It can be verified that in terms of the depth-averaged horizontal velocity \vec{u} , (A2) takes a simpler form:

$$\zeta_t + \nabla \cdot [(h + \epsilon \zeta) \vec{u}] = O(\mu^6) \quad (A10)$$

which is nothing but the depth-averaged law of continuity and is actually exact to all orders of μ^2 (Mei, 1989). But no significant simplification can be achieved for (A3) in terms of \vec{u} , and thus we choose to use Φ_0 and ζ as primary variables. Of course, ζ can be eliminated to yield a single equation for Φ_0 .

REFERENCES

- 1, Chen Y. and Liu P.L.-F. 1995: Modified Boussinesq Equations and Associated Parabolic Models for Water Wave Propagation, *J. Fluid Mech.*, 288, 351-381.
- 2, Greenspan D. and Casulli V. 1988: Numerical Analysis for Applied Mathematics, Science and Engineering, Addison-Wesley Publishing Company.
- 3, Liu P.L.-F. and Tasy T.K., 1984: Refraction-diffraction Model for Weakly Nonlinear Water Waves, *J. Fluid Mech.*, 141, 265-274.
- 4, Liu P.L.-F., Yoon S.B. and Kirby J. T., 1985: Nonlinear Refraction-diffraction of Waves in Shallow Water, *J. Fluid Mech.*, 153, 185-201.
- 5, Madsen P.A., Mei C.C. and Savarge R.P., 1970: The Evolution of Time-periodic Long Waves of Finite Amplitude, *J. Fluid Mech.*, 44, 195-208.
- 6, Madsen P.A. and Sørensen O.R., 1992: A New Form of the Boussinesq Equations with Improved Linear Dispersion Characteristics. Part 2. A Slowly-varying bathymetry. *Coastal Eng.*, 18, 182-204.
- 7, Mei C.C., 1989: *The Applied Dynamics of Ocean Surface Waves*, World Scientific.
- 8, Mei C. C. and Unluata U., 1972: Harmonic Generation in Shallow Water Waves, In *Waves on Beaches and Resulting Sediment Transport*, Meyer, R. E. (ed), Academic Press, New York, 181-202.
- 9, Nwogu O., 1993: Alternative form of Boussinesq Equations for Nearshore Wave Propagation, *J. Waterway, Port, Coastal & Ocean Eng.* ASCE, 119, 618-638.
- 10, Peregring D.H., 1967: Long Wave on a Beach. *J. Fluid Mech.*, 27, 815-827.
- 11, Radder A.C., 1979: On the parabolic equation Method for Water-wave Propagation, *J. Fluid Mech.*, 95, 159-176.
- 12, Rygg O. B., 1988: Nonlinear Refraction-diffraction of Surface Waves in Intermediate and Shallow Water, *Coastal Eng.*, 12, 191-211.
- 13, Wei G., Kirby J.T., Grilli S. T. and Subramanya R., 1995: A fully Nonlinear Boussinesq

Model for Surface Waves, Part I. Highly Nonlinear Unsteady Waves. J. Fluid Mech., 294, 71-92.
14, Whalin R. W., 1971: The Limit of Applicability of Linear Wave Refraction Theory in a
Convergence Zone. Res. Rep. H-71-3, US Army Corps of Eng, Waterways Exp. Station, Vicksburg,
MS.
15, Witting J.M., 1984: A Unified Model for the Evolution of Nonlinear Water Waves, J.
Comput. Phys., 56, 203-236.

If you want to read full text, please read PDF file.